Available online at www.sciencedirect.com
SCIENCE DIRECT
Journal of the European Ceramic Society 26 (2006) 1629–1635
www.elsevier.com/locate/jeurceramsoc

Densification, microstructural evolution and dielectric properties of $Ba_{6-3x}(Sm_{1-y}Nd_y)_{8+2x}Ti_{18}O_{54}$ microwave ceramics

Sea-Fue Wang [a,*], Yung-Fu Hsu [a], Yuh-Ruey Wang [a], Lung-Teng Cheng [a], Ya-Chi Hsu [a], Jinn P. Chu [b], Chi-Yuen Huang [c]

[a] *Department of Materials and Minerals Resources Engineering, National Taipei University of Technology, 1, Sec. 3, Chung-Hsaio E Rd., Taipei 106, Taiwan*
[b] *Institute of Materials Engineering, National Taiwan Ocean University, Keelung 202, Taiwan*
[c] *Department of Mineral and Petroleum Engineering, National Cheng Kung University, Tainan 701, Taiwan*

Received 30 December 2004; received in revised form 17 March 2005; accepted 26 March 2005
Available online 14 June 2005

Abstract

Utilizing different rare-earth cations R^{3+} to the $Ba_{6-3x}R_{8+2x}Ti_{18}O_{54}$ compounds is one of effective route to tailor the dielectric constant, quality factor and temperature coefficient of frequency. In this study, densification, microstructural evolution, and microwave dielectric properties of $Ba_{6-3x}(Sm_{1-y}Nd_y)_{8+2x}Ti_{18}O_{54}$ compound, with x ranging from 0.3 to 0.7; and y from 0 to 1.00, were investigated. The ceramics with $x = 0.7$ [$Ba_{3.9}(Sm_{1-y}Nd_y)_{9.4}Ti_{18}O_{54}$] has a higher densification compared with others, due to the formation of vacancy, in the perovskite-like tetragonal cavity of the tungsten bronze-type framework structure. Differential thermal analysis and density results show that the densification of $Ba_{6-3x}(Sm_yNd_{1-y})_{8+2x}Ti_{18}O_{54}$ ceramics during sintering is primarily resulting from the solid state sintering process. The phase homogeneity for the $Ba_{6-3x}(Sm_{0.5}Nd_{0.5})_{8+2x}Ti_{18}O_{54}$ system is at least extended in the range of x between 0.3 and 0.7. Combining different rare-earth cations appears not alter the single phase range in tungsten bronze-type $Ba_{6-3x}R_{8+2x}Ti_{18}O_{54}$ ceramics. The size of the columnar-grain in the microstructure increases with increasing the Nd/Sm ratio as well as the x value. Dielectric constant changes from 91.0 to 84.2 as the x increases from 0.3 to 0.7. Variation of the Nd/Sm ratio allows one to control the τ_f value to the nearly 0 ppm/°C.
© 2005 Elsevier Ltd. All rights reserved.

Keywords: Dielectric properties; Sintering; Grain size; $BaO–R_2O_3–TiO_2$; $(Ba,Sm)TiO_3$

1. Introduction

Commercial wireless communication has been a rapid growth market during the past decade. This technology advancement has been made possible, in part, with the recent revolution in the miniaturization of microwave circuits by using high dielectric constant (ε_r), low-loss (high Q) and temperature stable (low τ_f) dielectric resonators. Several ceramic materials, including $(Zr_{0.8}Sn_{0.2})TiO_4$, $Ba(Zn,Ta)O_3$, $BaTi_4O_9$, $Ba_2Ti_9O_{20}$, and $BaO–R_2O_3–TiO_2$ (R = rare earth ions) systems, have been developed for use as microwave resonators.[1–4] Among the various candidates, microwave dielectric ceramics based on the $BaO–R_2O_3–TiO_2$ are widely used in the electronics industry because of their high dielectric constants in the range of 80–110, good quality factors ($Q{\cdot}f$ over 5000 GHz), and a low temperature coefficient near zero.[4,5]

In the $BaO–R_2O_3–TiO_2$ system, various starting compositions (such as $BaO–R_2O_3–4TiO_2$, $BaO–R_2O_3–4.5TiO_2$, $0.15BaO–0.15R_2O_3–0.7TiO_2$ and $BaO–R_2O_3–5TiO_2$) and processing routes have resulted in the appearance of $Ba_{6-3x}R_{8+2x}Ti_{18}O_{54}$, $BaR_2Ti_4O_{12}$, and $BaR_2Ti_5O_{14}$, as well as the second phases including $BaTi_4O_9$, $Ba_2Ti_9O_{20}$, $R_2Ti_4O_{11}$, $R_4Ti_9O_{24}$, TiO_2, $R_2Ti_2O_7$, $RTiO_3$, and other barium polytitanates.[3,5–10] Ratios of various phases determine the microstructural evolution and dielectric properties. Although several $BaO–R_2O_3–TiO_2$ compounds

* Corresponding author. Tel.: +886 2 2771 2171; fax: +886 2 2771 2171.
E-mail address: sfwang@ntut.edu.tw (S.-F. Wang).

0955-2219/$ – see front matter © 2005 Elsevier Ltd. All rights reserved.
doi:10.1016/j.jeurceramsoc.2005.03.261

have been reported in the literature, a solid solution of $Ba_{6-3x}R_{8+2x}Ti_{18}O_{54}$, has received the most attention for its desirable microwave properties.[11] The $Ba_{6-3x}R_{8+2x}Ti_{18}O_{54}$, first found by Matveeva et al.,[12] has a tungsten bronze-type like structure. It is formed by TiO_6 octahedra sharing all apices with each other, and is characterized by distorted tetragonal and pentagonal tunnels running parallel to the c axis.[13] $Ba_{6-3x}R_{8+2x}Ti_{18}O_{54}$ solutions are existing on the tie line between $BaTiO_3$ and $R_2Ti_3O_9$ composition in the $BaO–R_2O_3–TiO_2$ ternary system.[14,15] The two extremity of the solid solutions ($x = 0, 1$) are corresponding to $3BaO–2R_2O_3–9TiO_2$ ($Ba_6R_8Ti_{18}O_{54}$) and $3BaO–5R_2O_3–18TiO_2$ ($Ba_3R_{10}Ti_{18}O_{54}$). $BaO–R_2O_3–4TiO_2$ ($BaR_2Ti_4O_{12}$) and $Ba_{3.75}R_{9.5}Ti_{18}O_{54}$ compounds are known as microwave resonator materials with $x = 0.5$ and 0.75 in the solid solution formula. $Ba_{6-3x}R_{8+2x}Ti_{18}O_{54}$ has three types of large cations sites including the largest one of pentagonal sites (A2), the medium one of rhombic sites (A1) in 2×2 perovskite blocks and the trigonal sites (C).[16,17] The trigonal C-sites are empty in this case. The main portion of A1 sites is occupied by R ions and a part of them is occupied by Ba according to the structural formula $[R_{8+2x}Ba_{2-3x}O_x]_{A1}[Ba_4]_{A2}Ti_{18}O_{54}$ $(2/3 \geq \times \geq 0)$.[13] Ohsato et al. reported that the $Q{\cdot}f$ changes non-linearly as a function of the composition x in the $Ba_{6-3x}R_{8+2x}Ti_{18}O_{54}$, formula, though ε_r and τ_f change linearly.[18] It was proposed that the non-linearity came from the site occupancy of large cations such as Ba and the rare earth ions. The $Q{\cdot}f$ exhibits the largest value at $x = 2/3$ in which Ba and R ions occupy separately A2 and A1 sites, respectively.[18]

To obtain high ε_r and $Q{\cdot}f$ value and near zero τ_f of $Ba_{6-3x}R_{8+2x}Ti_{18}O_{54}$ compounds, formation of multiphase ceramics by combining phases with τ_f value of the oppose sign,[6] doping by substitution alio- or isovalent ions, e.g. Bi or Pb for Ba,[20–22] or combining different rare earth cations R^{3+} under the formation of solid solutions in the single-phase state of the $Ba_{6-3x}[R'_yR''_{(1-y)}]_{8+2x}Ti_{18}O_{54}$ compounds[10,19,23,24] have been shown to be essential routes. Though the dielectric properties of $Ba_{6-3x}(R'_{1-y}R''_y)_{8+2x}Ti_{18}O_{54}$ system have been studied in the literature,[9,10,23–26] knowledge on the tailoring of the dielectric properties of these materials related to their densities and microstructures is still incomplete. In this study, a systematic investigation on the densification, microstructural evolution, and microwave dielectric properties of $Ba_{6-3x}(Sm_{1-y}Nd_y)_{8+2x}Ti_{18}O_{54}$ compound was performed.

2. Experimental procedure

$Ba_{6-3x}R_{8+2x}Ti_{18}O_{54}$ powders were prepared using the solid-state reaction technique. High purity (>99.9% purity) of TiO_2, $BaCO_3$, Sm_2O_3, and Nd_2O_3 (all Merck, Reagent grade) were used as raw materials. Oxides based on the compositions of $Ba_{6-3x}(Sm_{1-y}Nd_y)_{8+2x}Ti_{18}O_{54}$ ($x = 0.3$, 0.5, and 0.7; and $y = 0$, 0.25, 0.50, 0.75, and 1.00) were mixed and milled in methyl alcohol solution using polyethylene jars and zirconia balls for 24 h and then dried at 80 °C in an oven for overnight. After drying, the powders were calcined at 1150 °C for 4 h, and then re-milled in methyl alcohol for 8 h. The powders have particle size of ≈2.8 μm measured by light scattering (Zeta 1000) and surface area of ≈2.60 m^2/g from B.E.T. method. Phase identification on the calcined powders was performed using X-ray diffraction (XRD, Rigaku DMX-2200). The powder was added with a 5 wt.% of 15%-PVA solution and pressed into disc-shaped compacts using uniaxial pressure of 2 t/cm^2. The samples were then heat treated at 550 °C for 2 h to eliminate the PVA, followed by sintering at 1200, 1250, 1300, 1350, and 1400 °C for 8 h (heating rate = 10 °C/min).

Densities of specimens were measured using a liquid displacement method. X-ray diffraction was carried out on the ground powders of the sintered ceramics for phase identification. Scanning electron microscopy (SEM, Hitachi S4700), and energy dispersive spectroscopy (EDS) studies were performed on the sintered surfaces to characterize the microstructures and provide insight into reaction pathways. Differential thermal analysis (DTA) was performed using a Perkin-Elmer Calorimeter, Series 1700 DTA, on the samples to evaluate melting reactions.

The dielectric constants and unloaded Q values at microwave frequencies were measured in the $TE_{01\delta}$ mode using the Hakki and Colleman method[27] with a network analyzer (HP 8722ES). Measurements of the temperature coefficient of the resonance frequency τ_f were performed in the temperature range from 25 to 85 °C.

3. Results and discussion

The results of various $Ba_{6-3x}(Sm_{1-y}Nd_y)_{8+2x}Ti_{18}O_{54}$ compound with $x = 0.3$, 0.5, and 0.7; and $y = 0$, 0.25, 0.50, 0.75, and 1.00 are shown and discussed with respect to their densification, microstructural evolution, and dielectric properties.

3.1. Densification

The densities of the $Ba_{6-3x}(Sm_yNd_{1-y})_{8+2x}Ti_{18}O_{54}$ compounds sintered at different temperatures for x values equal to 0.3, 0.5, and 0.7 are shown in Fig. 1(a), (b), and (c), respectively. They are corresponding to the $Ba_{5.1}(Sm_yNd_{1-y})_{8.6}Ti_{18}O_{54}$, $Ba_{4.5}(Sm_yNd_{1-y})_9Ti_{18}O_{54}$, and $Ba_{3.9}(Sm_yNd_{1-y})_{9.4}Ti_{18}O_{54}$ compositions. The density increases considerably with the sintering temperature up to 1300 °C, then, levels off above this temperature. The trend of densification curves are consistent with those reported by Laffez et al.[26,28] and Ohsato et al.[23] Comparing the densification results for $y = 0$, 0.5, and 1.0 (corresponding to $Ba_{6-3x}Sm_{8+2x}Ti_{18}O_{54}$, $Ba_{6-3x}(Sm_{0.5}Nd_{0.5})_9Ti_{18}O_{54}$, and $Ba_{6-3x}Nd_{8+2x}Ti_{18}O_{54}$, respectively) shown in Fig. 1,

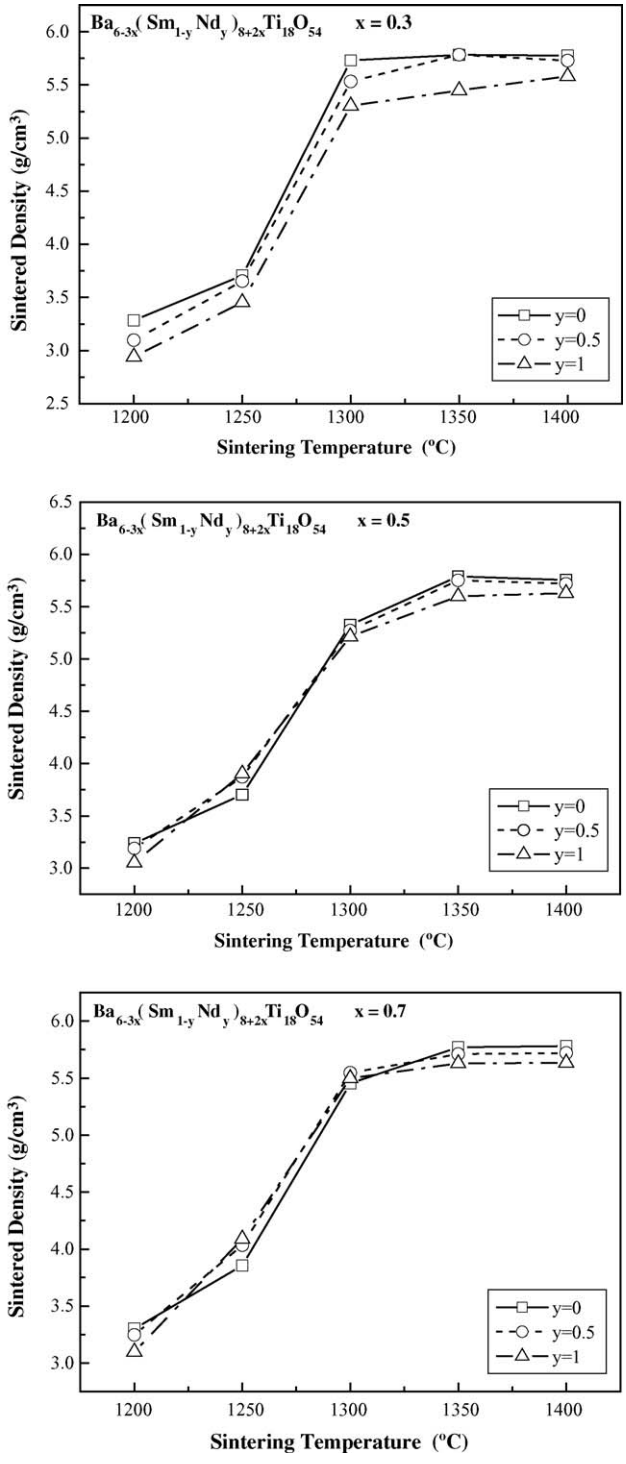

Fig. 1. The densities of the $Ba_{6-3x}(Sm_yNd_{1-y})_{8+2x}Ti_{18}O_{54}$ compounds sintered at different temperatures for (a) $y=0$, (b) $y=0.5$, and (c) $y=1.0$.

the ceramics with $y=0$ [$Ba_{6-3x}Sm_{8+2x}Ti_{18}O_{54}$] generally has a higher densification, and ceramics with $y=1.0$ [$Ba_{6-3x}Nd_{8+2x}Ti_{18}O_{54}$] are inferior to the others. The distinction is apparent for the $Ba_{5.1}(Sm_yNd_{1-y})_{8.6}Ti_{18}O_{54}$ system, particularly for the sintering temperatures above 1300 °C. This is due to the low theoretical density of

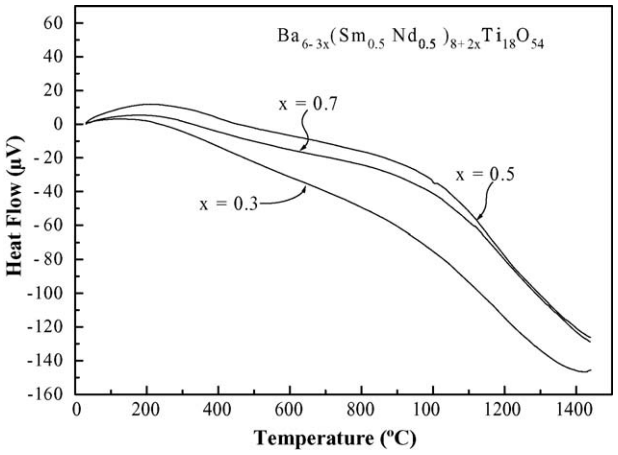

Fig. 2. DTA analysis of the $Ba_{6-3x}(Sm_{0.5}Nd_{0.5})_{8+2x}Ti_{18}O_{54}$ ceramics with $x=0.3$, 0.5, and 0.7, in an air atmosphere.

$Ba_{6-3x}Nd_{8+2x}Ti_{18}O_{54}$, which is derived from the large ionic radius of Nd^{3+} and the large unit cell volume.

In order to understand the possible melting reactions during the sintering process, DTA analysis was performed on the $Ba_{6-3x}(Sm_{0.5}Nd_{o.5})_{8+2x}Ti_{18}O_{54}$ ceramics with $x=0.3$, 0.5, and 0.7, in an air atmosphere. The results are shown in Fig. 2, which indicates no noticeable peak (a melting reaction) during heating for temperatures up to 1450 °C. It clarifies that the densification of $Ba_{6-3x}(Sm_yNd_{1-y})_{8+2x}Ti_{18}O_{54}$ ceramics during sintering is primarily resulting from the solid-state sintering process. This observation is different from those observed by Laffez et al.[28] and Ohsato et al.[29,30] Laffez et al.[28] showed that two endothermic peaks located at 1335 and 1350 °C in their DTA results for the $(BaO)_{0.15}(Sm_2O_3)_{0.15}(TiO_2)_{0.7}$ ceramics, which was proposed to be corresponding to oxygen absorption or desorption due to the transformation of second phase ($Ba_4Ti_{13}O_{30} \leftrightarrow Ba_6Ti_{17}O_{40}$) during sintering. Ohsato et al. showed that there is an endothermic reactions at 1350 °C for $BaSm_2Ti_4O_{12}$ ceramics and proposed that is corresponding to the eutectic reaction.[19,29] However, they later found that it is resulting from the $Sm_4O_3F_6$ instead of Sm_2O_3 in their starting raw materials which caused the synthesis composition slightly deviated toward TiO_2.[34] In this study, the formation of the $Ba_{6-3x}(Sm_yNd_{1-y})_{8+2x}Ti_{18}O_{54}$ is observed at temperature between 1000 and 1150 °C and the sintering proceeds rapidly above 1200 °C. Over 90% of the densification was performed below 1300 °C and maximum density was achieved when the temperature reaches 1350 °C (Fig. 1). It is not likely that any correlation between the sintering shrinkage and the endothermic peak of eutectic reaction at the temperature range of 1300–1350 °C, as reported in the literature.[5,29,30]

3.2. Phase formation and microstructural evolution

Various $Ba_{6-3x}(Sm_{1-y}Nd_y)_{8+2x}Ti_{18}O_{54}$ compositions after calcination at 1150 °C were characterized using XRD

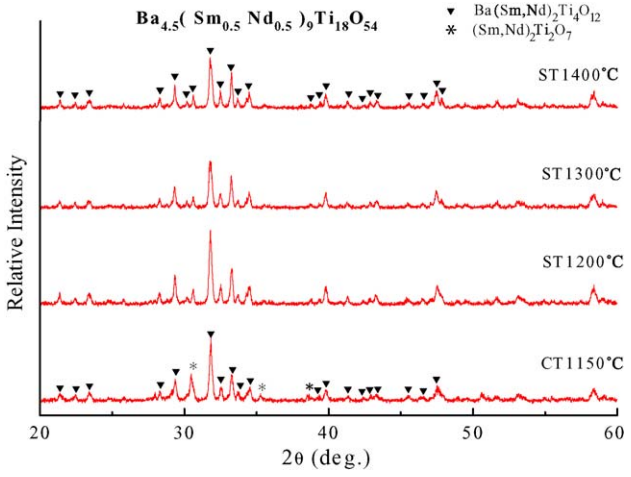

Fig. 3. A typical XRD patterns for the $Ba_{4.5}(Sm_{0.5}Nd_{0.5})_9Ti_{18}O_{54}$ system ($x = 0.5$ and $y = 0.5$) sintered at various temperatures.

analysis. The XRD patterns, which are nearly identical for all x and y values studied, show that they consist of a primary tungsten bronze-type $Ba_{6-3x}(Sm_{1-y}Nd_y)_{8+2x}Ti_{18}O_{54}$ phase, and a minor pyrochlore $(Sm,Nd)_2Ti_2O_7$ phase. No other detectable phases were found. Typical XRD patterns, the $Ba_{4.5}(Sm_{0.5}Nd_{0.5})_9Ti_{18}O_{54}$ system ($x = 0.5$ and $y = 0.5$) after calcinations as well as subsequently sintered at various temperatures, are shown in Fig. 3. At sintering temperatures above 1200 °C, a single phase of $Ba_{6-3x}(Sm_{1-y}Nd_y)_{8+2x}Ti_{18}O_{54}$ solid solution is observed. The difference in XRD patterns for $x = 0.3$, 0.5 and 0.7 of $Ba_{6-3x}(Sm_{0.5}Nd_{0.5})_{8+2x}Ti_{18}O_{54}$ system is not evident, as indicated in Fig. 4. The variations of lattice parameters with y compositions for the $Ba_{6-3x}(Sm_{1-y}Nd_y)_{8+2x}Ti_{18}O_{54}$ solid solution with $x = 0.3$, 0.5 and 0.7 are shown in Fig. 5. The lattice parameters increase almost linearly as the Nd/Sm ratio increases, due to the fact that the ionic radius of Nd^{3+} (1.123 Å) is larger than that of Sm^{3+} (1.098 Å). Similar trend is observed when the x value varies.

Ohsato et al.[34] have reported that the lattice parameters of the $Ba_{6-3x}Sm_{8+2x}Ti_{18}O_{54}$ and $Ba_{6-3x}Nd_{8+2x}Ti_{18}O_{54}$ compounds decrease as the x value increases. Our results in

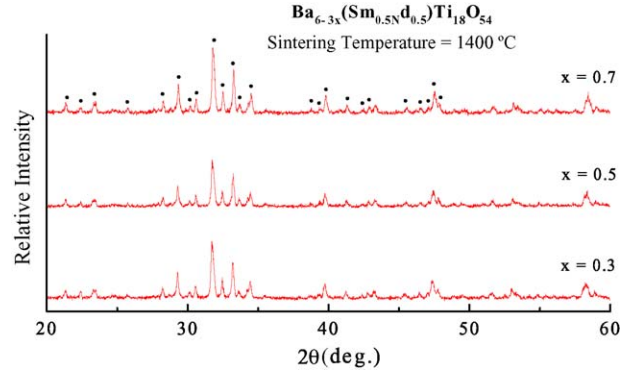

Fig. 4. XRD patterns for $Ba_{6-3x}(Sm_{0.5}Nd_{0.5})_{8+2x}Ti_{18}O_{54}$ ceramics, with $x = 0.3$, 0.5 and 0.7, sintered at 1400 °C.

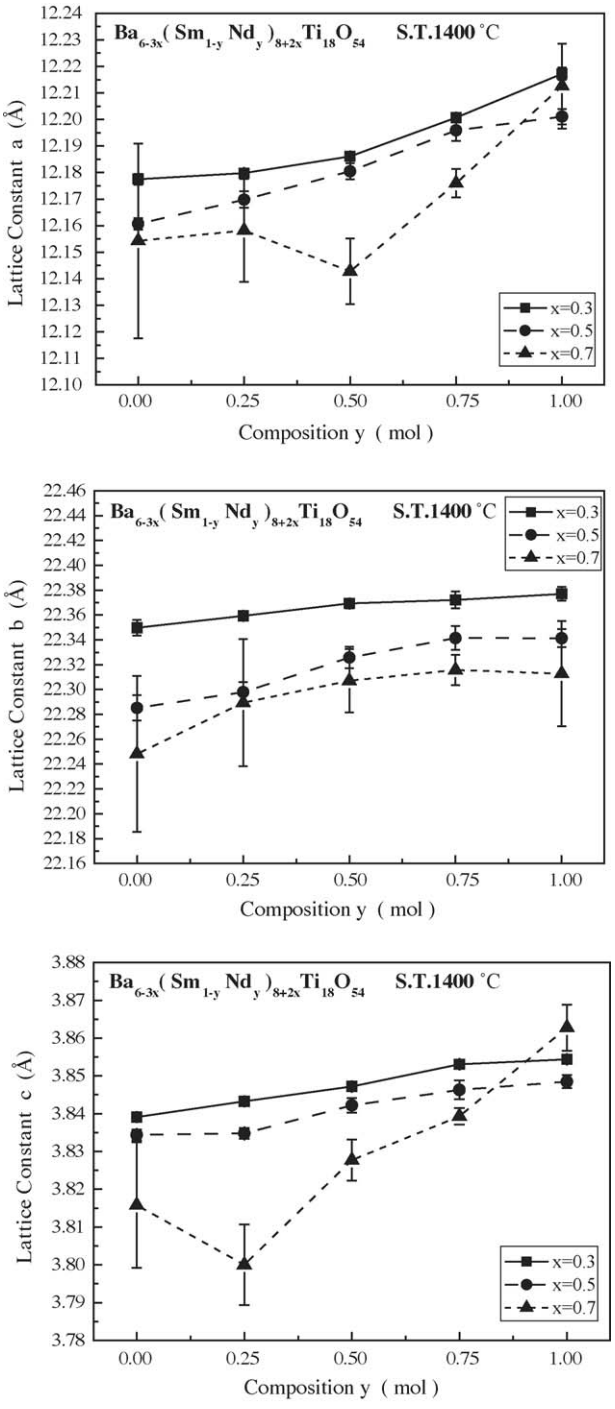

Fig. 5. The lattice parameters and unit cell volumes of the $Ba_{6-3x}(Sm_{1-y}Nd_y)_{8+2x}Ti_{18}O_{54}$ solid solution for $x = 0.3$, 0.5, and 0.7, as a function of y compositions.

Fig. 5 also show that the combination of Sm^{3+} and Nd^{3+} under the formation of $Ba_{6-3x}(Sm_{1-y}Nd_y)_{8+2x}Ti_{18}O_{54}$ solid solutions follows the same trend. For a given Nd/Sm ratio, the lattice parameters would decrease with increasing x value, which is derived from the substitution of the large Ba^{2+} by smaller R^{3+} as well as the associated formation of

vacancies. The unit cell volumes would increase with Nd/Sm ratio and decrease slightly with x value, as reported by Cruickshank et al.[14] Since no second phase is observed in these system, it manifests that the phase homogeneity for the $Ba_{6-3x}(Sm_{0.5}Nd_{0.5})_{8+2x}Ti_{18}O_{54}$ system is at least extended in the range of x between 0.3 and 0.7. This is generally in agreement with the results shown in the literature.[14,31] Ohsato et al.[31] showed that, for $Ba_{6-3x}Sm_{8+2x}Ti_{18}O_{54}$ ceramics, the single phase formation is confined to $0.3 < x < 0.7$. For $Ba_{6-3x}Nd_{8+2x}Ti_{18}O_{54}$ ceramics, Cruickshank et al.[14] showed that the solid solution is in the range of $0.25 < x < 0.75$ and, however, Ohsato et al.[31] reported that is in the range of $0 < x < 0.7$. They reported that $Sm_2Ti_2O_4$ and $R_4Ti_9O_{27}$ would form if x exceeds 0.7.[34] Based on our results, it seems that combining different rare-earth cations does not alter the single phase range in tungsten bronze-type $Ba_{6-3x}R_{8+2x}Ti_{18}O_{54}$ ceramics.

SEM micrographs of well-densified $Ba_{6-3x}(Sm_yNd_{1-y})_{8+2x}Ti_{18}O_{54}$ specimens with different Nd/Sm ratio for $x = 0.3$, 0.5 and 0.7, sintered at 1400 °C are shown in Fig. 6. In general they have a similar microstructure of columnar grains. It is consistent with those reported in the literature that the tungsten bronze phase tends to form a columnar structure.[32] The microstructural evolution confirms the observations of phases identified in the XRD patterns. Moreover, in Fig. 6, it is noticeable that the size of the columnar grain increases with increasing the Sm content as well as the x value. It seems that larger grain size is concurrent with higher densification (relative density). There is no visible second phase on the grain boundary which further confirm the densification of $Ba_{6-3x}(Sm_yNd_{1-y})_{8+2x}Ti_{18}O_{54}$ ceramics is primarily resulting from solid-state sintering, shown in the DTA and densification results (Figs. 1 and 2).

3.3. Dielectric properties

Generally, the dielectric properties are correlated to the density, microstructural evolution and composition of ceramics. In this study, the maximum densification is achieved at 1400 °C for all cases (Fig. 1). Therefore, the dielectric properties are compared for $Ba_{6-3x}(Sm_yNd_{1-y})_{8+2x}Ti_{18}O_{54}$ ceramics sintered at 1400 °C, to eliminate the porosity effects and any possible phase variation. Figs. 7 and 8 show the dielectric constant (ε_r), the product of quality factor and frequency ($Q{\cdot}f$) and the temperature coefficient of resonance frequency (τ_f) for $Ba_{6-3x}(Sm_yNd_{1-y})_{8+2x}Ti_{18}O_{54}$ ceramics with various Nd/Sm ratios for $x = 0.3$, 0.5, and 0.7. The dielectric constant increases with the Nd content and decreases with the x value. It varies from 88.5 to 94.9 for $x = 0.3$, from 81.6 to 91.0 for $x = 0.5$, and from 80.3 to 85.1 for $x = 0.7$. It is generally agreed that

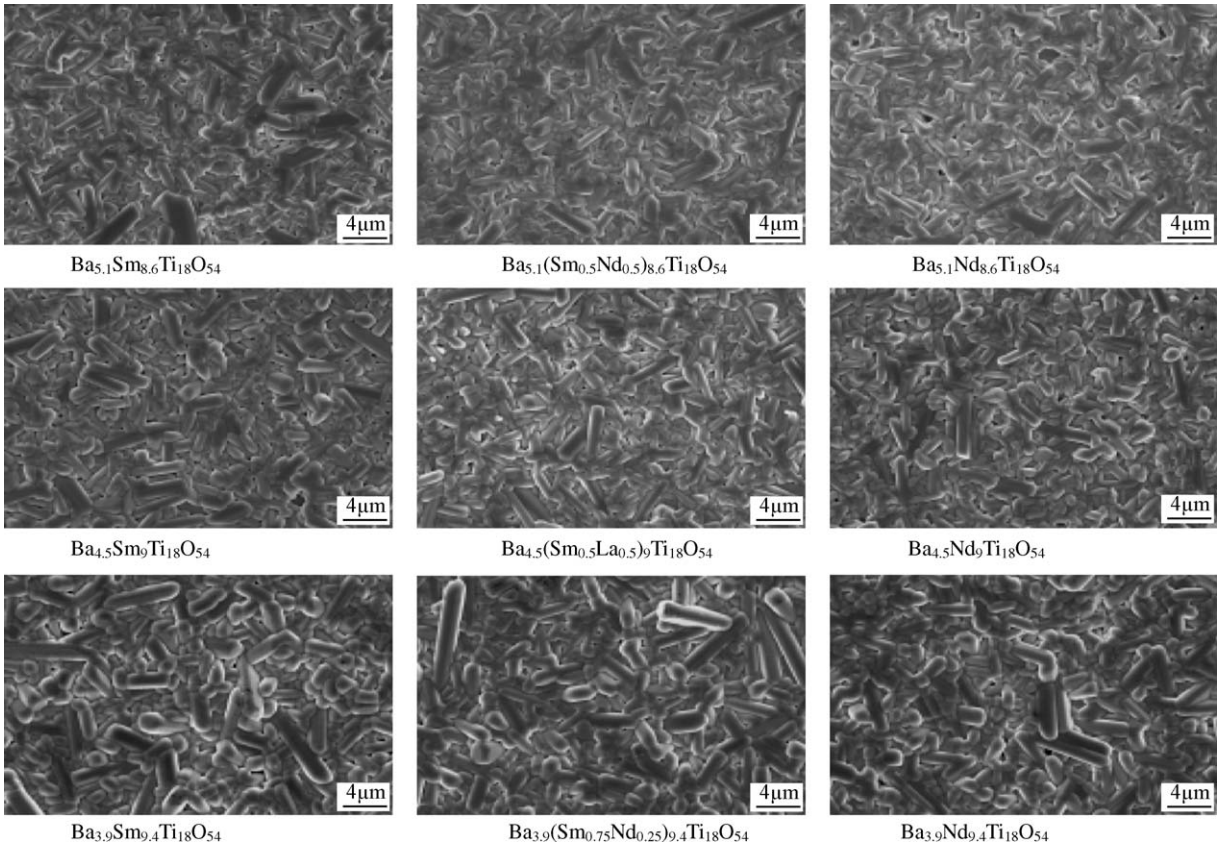

Fig. 6. SEM micrographs of $Ba_{6-3x}(Sm_yNd_{1-y})_{8+2x}Ti_{18}O_{54}$ specimens with different Nd/Sm ratio for $x = 0.3$, 0.5 and 0.7, sintered at 1400 °C.

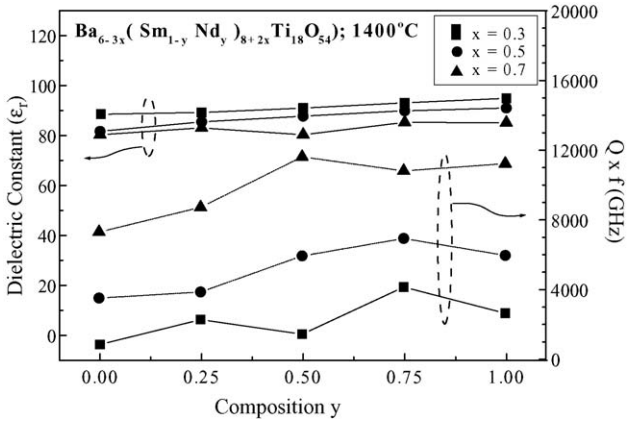

Fig. 7. (a) Dielectric constant (ε_r) and (b) the product of quality factor and frequency ($Q \times f$) of $Ba_{6-3x}(Sm_{0.5}Nd_{o.5})_{8+2x}Ti_{18}O_{54}$ ceramics with various Nd/Sm ratio for $x = 0.3$, 0.5, and 0.7, sintered at 1400 °C.

the dielectric constant for the tungsten bronze structure of $Ba_{6-3x}(Sm_yNd_{1-y})_{8+2x}Ti_{18}O_{54}$ is dependent on the ionic radius of the rare-earth cations. The large Nd^{3+} increases the unit cell volume and leads to the enlargement of the octahedral B site occupied by Ti^{4+} ions, which in turn, increases the allowed displacement of Ti^{4+} in the TiO_6 octahedron and raises the ionic electronic polarizability and the dielectric constant.[33,34] Regardless of the Nd/Sm ratio value, the dielectric constant decreases with the x value. For instance, the dielectric constants of $Ba_{6-3x}(Sm_{0.5}Nd_{o.5})_{8+2x}Ti_{18}O_{54}$ ceramics change from 91.0 to 84.2 as the x increases from 0.3 to 0.7. This is due to the facts that the volume contraction of $Ba_{6-3x}(Sm_yNd_{1-y})_{8+2x}Ti_{18}O_{54}$ unit cell resulting from the vacancy formation ($3Ba^{2+} \rightarrow 2R^{3+} + \square$),[14] smaller ionic radius of R^{3+} compared with Ba^{2+} in the rhombic sites, as well as the lower electronic polarization due to the lower electronic polarizability of rare earth elements as the x increases (more

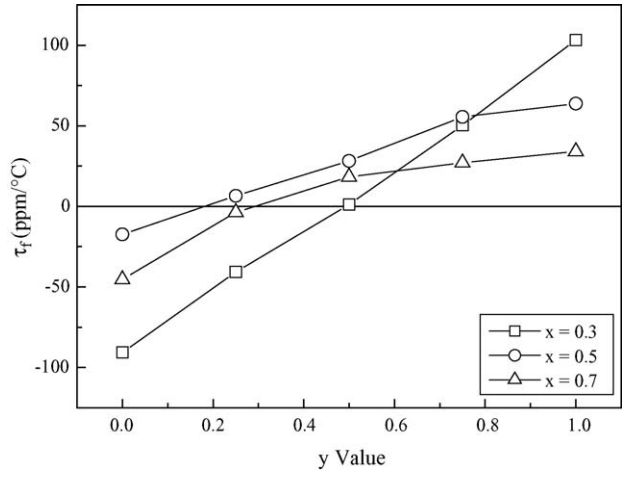

Fig. 8. Temperature coefficient of resonance frequency (τ_f) of $Ba_{6-3x}(Sm_{0.5}Nd_{o.5})_{8+2x}Ti_{18}O_{54}$ ceramics with various Nd/Sm ratio for $x = 0.3$, 0.5, and 0.7, sintered at 1400 °C.

Ba^{2+} replaced by R^{3+}).[5] The $Q{\cdot}f$ value generally varies non-linearly with compositions.[18,30] It has a similar trend with that of the dielectric constant, as shown in Fig. 7. The $Q{\cdot}f$ values seem to be larger as the Nd/Sm ratio in compositions increases.

Fluctuations of τ_f for a given composition are often observed in the literature, since it is closely related to the sintering profile and microstructural evolution. τ_f value of a multiphase could be estimated by the temperature coefficient of resonant frequency and volume fraction of the existing individual phase.[6] In Fig. 8, the τ_f shows a continuous variation from negative to positives values as the y increases. Variation of the Nd/Sm ratio allows one to control the τ_f value to the nearly 0 ppm/°C, similar to that reported in the literature.[6] Starting from negative values of τ_f, the zero line is cut out for $x = 0.3$ series in the vicinity of $y = 0.5$, for $x = 0.5$ series at about $y = 0.18$ and for $x = 0.7$ series near $y = 0.28$. As the x increases, the slope of the τ_f value versus the Nd/Sm ratio becomes small and the τ_f values approach the zero line.

4. Summary

This study shows the densification, microstructural evolution, and microwave dielectric properties of $Ba_{6-3x}(Sm_{1-y}Nd_y)_{8+2x}Ti_{18}O_{54}$ compounds, with $x = 0.3$, 0.5, and 0.7; and $y = 0$, 0.25, 0.50, 0.75, and 1.00. Several important results are obtained as followed:

1. The ceramics with $x = 0.7$ [$Ba_{3.9}(Sm_{1-y}Nd_y)_{9.4}Ti_{18}O_{54}$] have a higher densification compared with $x = 0.5$ [$Ba_{4.5}(Sm_{1-y}Nd_y)_9Ti_{18}O_{54}$] and $x = 0.3$ [$Ba_{5.1}(Sm_{1-y}Nd_y)_{8+2x}Ti_{18}O_{54}$], which may be due to the formation of vacancy in the perovskite-like tetragonal cavity of the tungsten bronze-type framework structure as x increases.
2. No evidence of liquid phase formation was observed during sintering of $Ba_{6-3x}(Sm_yNd_{1-y})_{8+2x}Ti_{18}O_{54}$ ceramics. The densification of the ceramics is primarily resulting from the solid-state sintering process.
3. Combining different rare-earth cations seems not alter the single-phase range in tungsten bronze-type $Ba_{6-3x}R_{8+2x}Ti_{18}O_{54}$ ceramics. They possess a similar columnar-grains microstructure. At a given sintering temperature, the columnar-grain size increases with increasing the Nd/Sm ratio as well as the x value.
4. A τ_f value with near 0 ppm/°C can be obtained by altering the Nd/Sm ratio. The τ_f shows a continuous variation from negative to positives values as the y increases. The zero τ_f line is cut out for $x = 0.3$ series in the vicinity of $y = 0.5$, for $x = 0.5$ series at about $y = 0.18$ and for $x = 0.7$ series near $y = 0.28$. As the x increases, the slope of the τ_f value versus the Nd/Sm ratio of ceramic becomes less.

References

1. O'Bryan, Jr. H. M., Plourde, J. K. and Thomson, Jr. J., Dielectric for Microwave Application, U.S. Patent 4,563,661 (1986).
2. Kolar, D., Stadler, Z., Gaberscek, S. and Suvorov, D., Ceramic and dielectric properties of selected compositions in the $BaO–TiO_2–Nd_2O_3$ system. *Ber. Dr. Keram. Ges.*, 1978, **55**, 346–347.
3. Kolar, D., Gaberscek, S. and Volavsek, B., Synthesis and crystal chemistry of $BaNdTi_3O_{10}$, $BaNd_2Ti_5O_{14}$, and $Nd_4Ti_5O_{24}$. *J. Solid State Chem.*, 1981, **38**, 58–164.
4. Ohsato, H., Science of tungstenbronze-type like $Ba_{6-3x}R_{8+2x}Ti_{18}O_{54}$ (R = rare earth) microwave dielectric solid solutions. *J. Euro. Ceram. Soc.*, 2001, **21**, 2701–2711.
5. Nishigaki, S., Karo, H., Yano, S. and Kamimura, R., Microwave dielectric properties of $(Ba,Sr)O–Sm_2O_3–TiO_2$ ceramics. *Am. Ceram. Soc. Bull.*, 1987, **66**, 1405–1410.
6. Fukuda, K., Kitoh, R. and Awai, I., Microwave characteristics of mixed phases of $BaPr_2Ti_4O_{12}–BaPr_2Ti_5O_{l4}$ ceramics. *J. Mater. Res.*, 1995, **10**, 312–319.
7. Kim, T. H., Park, J. R., Lee, S. J., Sung, H. K., Lee, S. S. and Choy, T. G., Effects of Nd_2O_3 and TiO_2 addition on the microwave dielectric properties of $BaO–Nd_2O_3–TiO_2$ System. *ETRI J.*, 1996, **18**(1), 15–27.
8. Sreemoolanadhan, H., Sebastian, M. T. and Mohanan, P., Dielectric resonators in $BaO–Ln_2O_3–5TiO_2$ system (Ln = La, Pr, Nd, Sm). *Br. Ceram. Trans.*, 1996, **95**(2), 79–81.
9. Webhofer, A. and Feltz, A., Microwave dielectric properties of ceramics of the system $Ba_{6-x}(Sm_yNd_{1-y})_{8+2x/3}$. *J. Mate. Sci. Lett.*, 1999, **18**, 719–721.
10. Mercurio, J. P., Manier, M. and Frit, B., Microwave dielectric properties of $BaNd_{2(1-x)}Sm_{2x}Ti_5O_{14}$ ceramics. *Mater. Lett.*, 1989, **8**(3–4), 112–114.
11. Azough, F., Setasuwon, P. and Freer, R., The structure and microwave dielectric properties of ceramics based on $Ba_{3.75}Nd_{9.5}Ti_{18}O_{54}$. Material and processes for wireless communications. *Ceram. Trans.*, 1995, **53**, 215–226.
12. Matveeva, R. G., Varforomeev, M. B. and ll'yuschenko, L. S., Refinement of the composition crystal structure of $Ba_{3.75}Pr_{9.5}Ti_{18}O_{54}$. *Zh. Neorg. Khim.*, 1984, **29**, 31–34;
    Matveeva, R. G., Varforomeev, M. B. and ll'yuschenko, L. S., Refinement of the composition crystal structure of $Ba_{3.75}Pr_{9.5}Ti_{18}O_{54}$. *Trans. Russ. J. Inorg. Chem.*, 1984, **29**, 31–34.
13. Okudera, H., Nakamura, M., Toraya, H. and Ohsato, H., Tungsten bronze-type solid solutions $Ba_{6-3x}R_{8+2x}Ti_{18}O_{54}$ ($x = 0.3$, 0.5, 0.67, 0.71) with superstructure. *J. Solid State Chem.*, 1999, **142**, 336–343.
14. Cruickshank, K. M., Jang, X., Wood, G., Lachowski, W. E. and West, A. R., *J. Am. Ceram. Soc.*, 1996, **79**, 1605.
15. Varfolomeev, M. B., Mironov, A. S., Kostomarov, V. S., Golubtsova, L. A. and Zolotova, T. A., The synthesis and homogeneity ranges of the phases $Ba_{6-3x}R_{8+2x/3}Ti_{18}O_{54}$. *Russ. J. Inorg. Chem.*, 1988, **33**, 607–608.
16. Rawn, C. J., BirnieIll, D. P., Bruck, M. A., Enemark, J. H. and Roth, R. S., Structural investigation of $Ba_{6-3x}Ln_{8+2x}Ti_{18}O_{54}$ ($x = 0.27$, Ln = Sm) by single crystal X-ray diffraction in space group *Pnma* (No. 62). *J. Mater. Res.*, 1998, **13**(1), 187–196.
17. Ubic, R., Reaney, I. M. and Lee, W. E., Space group determination of $Ba_{6-3x}R_{8+2x}Ti_{18}O_{54}$. *J. Am. Ceram. Soc.*, 1999, **82**, 1336–1338.
18. Ohsato, H. and Imaeda, M., The quality factor of the microwave dielectric materials based on the crystal structure-as an example: the $Ba_{6-3x}R_{8+2x}Ti_{18}O_{54}$ (R = rare earth) solid solutions. *Mater. Chem. Phys.*, 2003, **79**, 208–212.
19. Toraya, H., Whole-powder-pattern fitting without reference to a structural model: application to X-ray powder diffractometer data. *J. Appl. Cryst.*, 1986, **19**, 440–447.
20. Valant, M., Suvorov, D. and Kolar, D., Role of Bi_2O_3 in optimizing the dielectric properties of $Ba_{4.5}Nd_9Ti_{18}O_{54}$ based microwave ceramics. *J. Mater. Res.*, 1996, **11**(4), 928–931.
21. Nenasheva, E. A. and Kartenko, N. F., High dielectric constant microwave ceramics. *J. Euro. Ceram. Soc.*, 2001, **21**, 2697–2701.
22. Wu, Y. J. and Chen, X. M., Structure and microwave dielectric properties of $Ba_{6-3x}(Nd,Bi_y)_{8+2x}Ti_{18}O_{54}$ ($x + 2/3$) solid solution. *J. Mater. Res.*, 2001, **16**(6), 1734–1738.
23. Ohsato, H., Kato, H., Mizuta, M., Nishigaki, S. and Okuda, T., Microwave dielectric properties of the $Ba_{6-3x}(Sm_{1-y}R_y)_{8+2x}Ti_{18}O_{54}$ (R = Nd, La) solid solutions with zero temperature coefficient of the resonant frequency. *Jpn. J. Appl. Phys.*, 1995, **34**, 5413–5417.
24. Wu, Y. J. and Chen, X. M., Bismuth/samarium cosubstituted $Ba_{6-3x}R_{8+2x}Ti_{18}O_{54}$ microwave dielectric ceramics. *J. Am. Ceram. Soc.*, 2000, **83**(7), 1837–1839.
25. Belous, A. G. and Ovchar, O. V., MW dielectrics with perovskite-like structure based on Sm-containing system. *J. Eur. Ceram. Soc.*, 1999, **19**, 1119–1122.
26. Laffez, P., Desgardin, G. and Raveac, B., Microwave dielectric properties of doped $Ba_{6-x}(Sm_yNd_{1-y})_{8+2x/3}Ti_{18}O_{54}$ oxides. *J. Mater. Sci.*, 1995, **30**, 267–273.
27. Hakki, B. W. and Coleman, P. D., A Dielectric resonator method of measuring inductive in the millimeter range. *IRE Trans. Microwave Theory Tech., MTT-8*, 1960, 402–410.
28. Laffez, P., Desgardin, G. and Raveac, B., Influence of calcination, sintering and composition upon microwave properties of the $Ba_{6-x}Sm_{8+2x/3}Ti_{18}O_{54}$ type oxide. *J. Mater. Sci.*, 1992, **27**, 5229–5238.
29. Ohsato, H., Nishigaki, S. and Okuda, T., Superlattice and dielectric properties of dielectric compounds. *Jpn. J. Appl. Phys.*, 1992, **31**, 3136–3138.
30. Ohsato, H., Ohhashi, T., Kato, H., Nishigaki, S. and Okuda, T., Microwave dielectric properties and structure of the $Ba_{6-3x}Sm_{8+2x}Ti_{18}O_{54}$ solid solutions. *Jpn. J. Appl. Phys.*, 1995, **34**, 187–191.
31. Ohsato, H., Ohhashi, T., Nishigaki, S., Okuda, T., Sumiya, K. and Suzuki, S., Formation of solid solution of new tungsten bronze-type microwave dielectric compounds $Ba_{6-3x}R_{8+2x}Ti_{18}O_{54}$ (R = Nd and Sm, $0 \leqq x \leqq 1$). *Jpn. J. Appl. Phys.*, 1993, **32**, 4323–4326.
32. Zheng, X. H. and Chen, X. M., Effect of Sr substitution on dielectric characteristics of $Ba_4Nd_2Ti_4Ta_6O_{30}$ ceramics. *Jpn. J. Appl. Phys.*, 2001, **40**(6A), 4114–4117.
33. Valant, M., Suvorov, D. and Rawn, C. J., Intrinsic reasons for variations in dielectric properties of $Ba_{6-3x}R_{8+2x}Ti_{18}O_{54}$ (R = La–Gd) solid solutions. *Jpn. J. Appl. Phys*, 1999, **38**, 2820–2826.
34. Ohsato, H., Mizuta, M., Ikoma, T., Onogi, Z., Nishigaki, S. and Okuda, T., Microwave dielectric properties of tungsten bronze-type $Ba_{6-3x}R_{8+2x}Ti_{18}O_{54}$ (R = La, Pr, Nd and Sm) solid solutions. *J. Ceram. Soc. Jpn.*, 1998, **106**(2), 178–182.